

Synthetic Aperture Radar Imaging of Ocean Waves: Comparison With Wave Measurements

WILLIAM MCLEISH,¹ DUNCAN ROSS,¹ ROBERT A. SHUCHMAN,² PAUL G. TELEKI,³
S. VINCENT HSIAO,⁴ O. H. SHEMDIN,⁴ AND W. E. BROWN, JR.⁴

Synthetic aperture radar images of ocean waves were obtained in conjunction with reference wave data near Marineland, Florida, December 14, 1975. Each of the various types of measurements were processed into a form that allowed direct comparisons with the others. Maxima of radar spectra occurred at the same frequencies as the maxima of reference wave height spectra. In a comparison of a radar spectrum with observed spectra of wave height, wave orbital velocity, and surface slope the high-frequency portion of the radar spectrum lay near and between the wave height and the orbital velocity spectra but differed significantly from the surface slope spectrum. The radar-derived mean directions and model-fitted directional spreads of wave energy were close to the values from a directional wave buoy and indicated the accuracy of radar measurements of wave direction. However, a directional plot of a radar spectrum near shore at the frequency of the maximum showed a sharper peak than such a plot of a fitted spectrum derived from reference data. The high directional resolution of the radar, in addition to its making observations at different locations, allowed radar images to provide information about ocean waves not available from the other instruments. As a swell propagated across the continental shelf, it was scattered in direction, apparently by the irregularities of the bottom, and very little of its energy reached shore. The shorter sea waves had a narrow directional distribution when first observed offshore that may have been sharpened by interaction with the Gulf Stream. Radar images showed effects of bottom refraction on the sea waves as they moved into progressively shallower water.

INTRODUCTION

The ability to obtain nearly synoptic directional wave information on a relatively large spatial scale is a goal actively pursued by some in the ocean research community. One approach to obtaining such information is through the use of imaging radar. *Crombie* [1955] was the first to associate radar backscatter with ocean waves with a wavelength of one-half the wavelength of the incident radar. *Wright* [1968] and *Bass et al.* [1968] proposed a composite theory wherein the level of backscatter was a function of the amplitude of the short (Bragg) waves and their local tilt due to the presence of an underlying longer wave. Thus if a radar beam properly scans the surface, theory predicts that the underlying waves will be imaged.

Indeed, real aperture radars have been in use since the mid-1950's by the Dutch to observe swell patterns at the entrances to harbors, and airborne systems have been utilized both by the Dutch [*De Loor and Brunsveld Van Hulst*, 1978] and in the USSR [*Bondarenko et al.*, 1972] since the early 1970's. Airborne synthetic aperture radar has been used to observe waves generated by hurricanes at L band [*Ross et al.*, 1974], while X band systems have observed features of the Gulf Stream [*Wright et al.*, 1976].

The Seasat A satellite was the first attempt to obtain wave imagery from space. Preliminary results from its data [*Gonzalez et al.*, 1979; *Teleki et al.*, 1979] show that useful imagery can be obtained.

The Seasat A results and previous studies were principally

¹ Sea-Air Interaction Laboratory, National Oceanic and Atmospheric Administration, Miami, Florida 33149.

² Environmental Research Institute of Michigan, Ann Arbor, Michigan 48107.

³ U.S. Geological Survey, Reston, Virginia 22092.

⁴ Jet Propulsion Laboratory, California Institute of Technology, Pasadena, California 91103.

This paper is not subject to U.S. copyright. Published in 1980 by the American Geophysical Union.

concerned with wavelength and direction information. The results are encouraging, but it must be noted that the majority of waves imaged appear to have been swell and the limitations of the synthetic aperture approach in imaging local sea is not known.

According to the theory of synthetic aperture systems, as discussed by *Brown and Porcello* [1969], the location of a reflecting element on the earth's surface is determined by tracking the Doppler phase history of the returned signal. For a fixed surface, there is a unique Doppler relationship for the received radar signal from a given earth location. If the surface is in motion, however, as in the case of ocean waves, the Doppler history of the earth location is distorted, and the resulting image becomes 'defocused.' The amount of defocusing varies with the speed of the motions [*Alpers and Rufenach*, 1979].

In this paper we examine synthetic aperture imagery of ocean waves and compare characteristics of the derived radar spectra with wave spectra obtained from in situ instrumentation. Thus the frequency and directional properties of radar spectra are compared with those of height, orbital velocity, and slope spectra obtained from a buoy, orthogonally oriented current meters, pressure transducers, and an airborne laser wave profilometer. The different instruments were assembled in a joint experiment held off Marineland, Florida, in December 1975. The waves on that date had been generated over a fetch of 500-1000 km by a nearly steady east wind with a speed of about 10 m/s offshore and 3 m/s near the coast. Thus the offshore waves were in the downwind portion of an extended generating area, whereas those near shore had begun a modification toward swell under the decreased wind speeds. Propagation through the Gulf Stream and in shallow water caused additional changes in the waves.

The results of the study are both encouraging and inconclusive. The transfer function relating variations in the radar return signal to ocean waves depends in an as yet undetermined manner on several variables, including the state of the

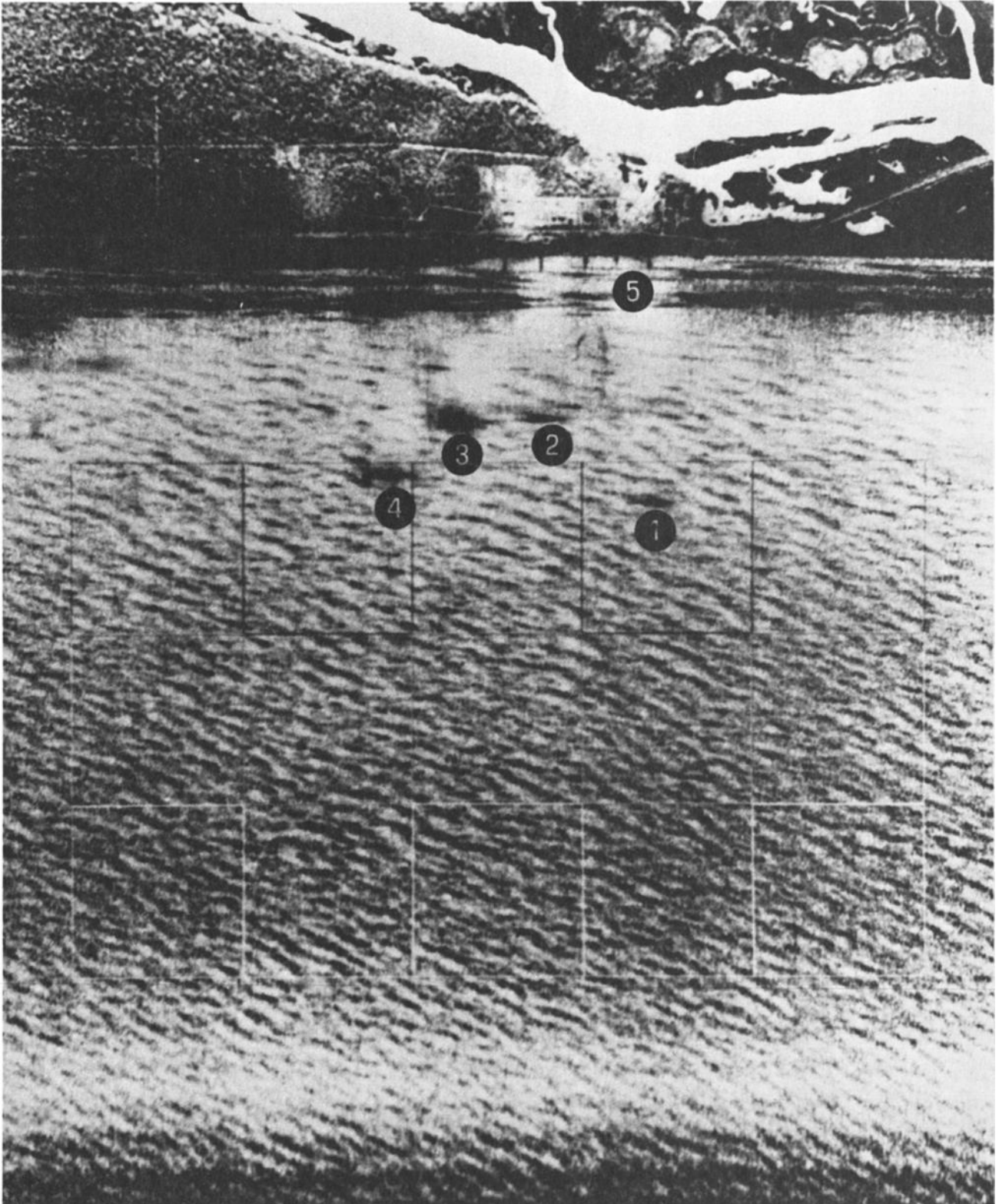


Fig. 1. Radar image of ocean waves near shore and reference wave measuring instruments: (1) ship operating pitch-roll buoy, (2) UF wave-recording tower, (3) ship operating wave tower, (4) ship recording background data, and (5) surf and five groins extending from the beach. The sea sled was inshore of the pitch-roll buoy. The 15 squares are the regions of individual radar spectra, where each side represents 683 m.

sea, the aspect angle from which the waves are viewed, and the operating characteristics of the radar. Thus no single study is likely to provide a satisfactory knowledge of the function. We are, however, more knowledgeable than we were before

and believe that the cumulative results will lead to the capability of observing remotely the complete two-dimensional wave energy spectrum when in conjunction with a reference airborne wave-measuring instrument.

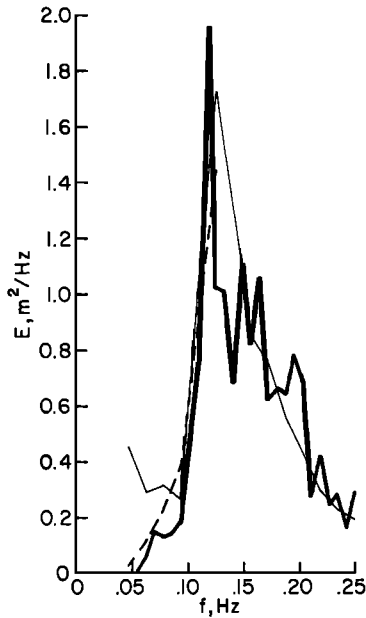


Fig. 2. Intercomparison among reference wave height spectrum measurements: pitch-roll buoy (light solid curve), UF tower (heavy solid curve), and sea sled (dashed curve). E is variance density.

Preliminary portions of the present results were included in the studies by *Shemdin et al.* [1978a], *Hsiao* [1978], and *Teleki et al.* [1978].

RADAR WAVE MEASUREMENTS

Images of ocean waves were recorded by an X and L band airborne synthetic aperture radar viewing the sea surface at large depression angles [Shemdin et al., 1978a]. In the present study, only horizontally polarized X band ($\lambda = 3.2$ cm) radar data obtained on December 14, 1975, are examined. The radar images showed that the ocean waves were traveling in a direction about 20° – 30° from the range direction. Theoretical considerations suggest that range-traveling waves give optimum patterns on synthetic aperture radar images [Shuchman and Zelenka, 1978]. The radar image in Figure 1 shows ocean waves near shore, the areas of radar image analysis, and the locations of the reference instruments. Since the waves in the areas of radar analysis appear to be similar to those at the locations of the reference instruments, comparison of the results is considered to be appropriate.

An image film was obtained from the radar signal film through an optical Fourier transform [Shuchman and Zelenka, 1978]. Measurements of the optical transmissivity of the image film over the areas marked in Figure 1 produced sets of digital data. An offset weighted filter was used to correct for the distortion resulting from the slant range-ground range difference.

Two-dimensional Fourier transforms of geometry-corrected digital data were calculated by a fast Fourier transform technique after the method of *Rabiner and Gold* [1975]. According to this method the transforms are given by

$$F(k_1, k_2) = \sum_m \sum_n A_{mn} e^{ik_1 x_m} e^{ik_2 x_n} \quad (1)$$

where k_1 and k_2 are orthogonal components of wave number k , $k_1^2 + k_2^2 = k^2$, $k = 2\pi/L$, L is the wavelength, and each A_{mn}

is the optical transmissivity at an image location. Wave number spectra were obtained with

$$S(k_1, k_2) = |F(k_1, k_2)|^2 / (\Delta k_1 \Delta k_2) \quad (2)$$

The propagation of waves while they are being scanned by a moving sensor may introduce a significant distortion into the record. The effects of wave motion on spectra derived from several types of measurements were examined by *Long* [1979]. The wind caused a lateral motion of the aircraft, but its effect on the results of the radar measurements was negligible in the present experiment. Under these conditions, *Long's* equations show that each component of the spectrum is shifted aft by a distance

$$\Delta k_1 = -k \cdot (c/v) \quad (3)$$

where c is the phase speed of the waves at that wave number and water depth and v is the aircraft speed. The change in the wave number of an estimate causes a change in the density of that estimate given by

$$\Delta S/S = \frac{1}{2}(c/v) \cos \alpha \quad (4)$$

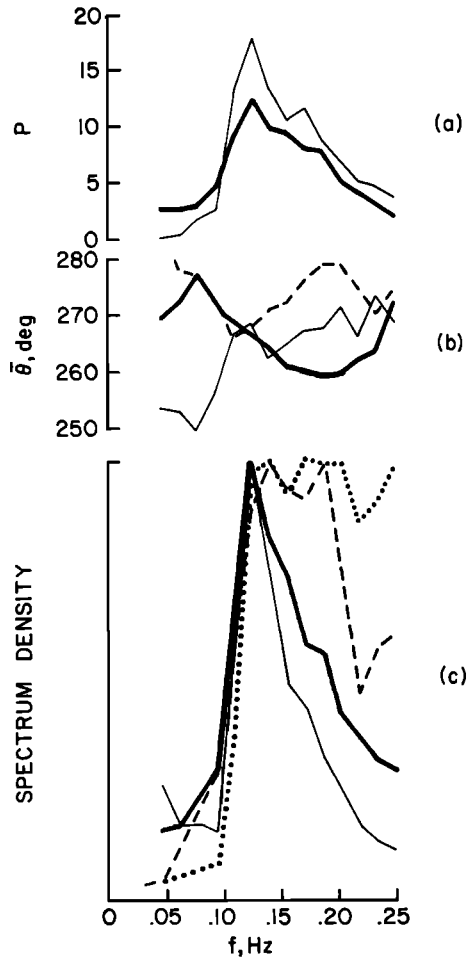


Fig. 3. Calculations from radar data (heavy solid curves) compared with those from reference instruments. (a) Cosine spread exponent factor $P(f)$. (b) Mean direction $\theta(f)$, same instrument designation as below. (c) Wave height spectrum from pitch-roll buoy acceleration (light solid curve), peak at $1.73 \text{ m}^2/\text{Hz}$; orbital velocity spectrum from sea sled (dashed curve), peak value is $1.30 \text{ cm}^2 \text{ s}^{-2} \text{ Hz}^{-1}$; and surface slope spectrum from pitch-roll buoy tilt (dotted curve), peak value is $0.0127 \text{ rad}^2/\text{Hz}$.

where α is the angle between aircraft and wave propagation directions. These two effects were removed prior to further calculation.

One-dimensional wave number spectra were calculated with

$$S(k) = \sum_{n=1}^{179} S(k, \theta_n) k \Delta\theta \quad (5)$$

where $S(k, \theta_n) = S(k_1, k_2)$ with $k_1 = k \sin \theta_n$, $k_2 = k \cos \theta_n$, $\theta_n = \theta_{n-1} + \Delta\theta$, and $\Delta\theta = 1^\circ$. The initial values of θ_n were selected in order to include those portions of the two-dimensional spectra that occurred within 90° of selected dominant wave directions.

Frequency spectra were obtained from wave number spectra by using the transformation

$$S(f) = S(k) \Delta k / \Delta f \quad (6)$$

where Δk and Δf are the differences between the boundaries of spectrum estimates. More stable spectra were obtained by combining the results of 15 adjacent squares in each image. The amplitudes of these spectra were normalized with respect to those of the reference spectra at the peak frequencies.

Directional properties of the waves recorded by the radar were examined following the approach given by *Longuet-Higgins et al.* [1963]. For each value of f evaluated, the first two Fourier harmonics of $S(k, \theta_n)$ were calculated by direct transformation with

$$a_1 + ib_1 = \frac{1}{T} \sum_{n=1}^{179} S(k, \theta_n) \cos \theta_n + \frac{i}{T} \sum_{n=1}^{179} S(k, \theta_n) \sin \theta_n \quad (7)$$

$$a_2 + ib_2 = \frac{1}{T} \sum_{n=1}^{179} S(k, \theta_n) \cos 2\theta_n + \frac{i}{T} \sum_{n=1}^{179} S(k, \theta_n) \sin 2\theta_n \quad (8)$$

where

$$T = \sum_{n=1}^{179} S(k, \theta_n)$$

A smoothed directional distribution function was calculated with

$$G(\theta) = \frac{1}{2} + \frac{2}{3} (a_1 \cos \theta + b_1 \sin \theta) + \frac{1}{6} (a_2 \cos 2\theta + b_2 \sin 2\theta) \quad (9)$$

and the mean direction was obtained with

$$\bar{\theta} = \tan^{-1}(b_1/a_1) \quad (10)$$

The exponent factor of a cosine fit to the directional distribution of the form

$$E(\theta) = \cos^{2PU} \frac{1}{2}(\theta - \bar{\theta}) \quad (11)$$

was approximated following *Mitsuyasu et al.* [1975] with

$$P(f) = 1/[1 - (a_1^2 + b_1^2)^{1/2}] - 1 \quad (12)$$

REFERENCE WAVE MEASUREMENTS

A pitch-roll buoy similar to one described by *Longuet-Higgins et al.* [1963] was operated on December 14, 1975, in approximately 10-m water depth at the location shown in Figure 1. A series of nine consecutive 34-min records were processed. During the 5 hours of measurement, no significant changes in the wave properties were found; hence the data were com-

pared in one calculation. Estimates at groups of adjacent frequencies were averaged to produce a spectrum with more than 500 degrees of freedom. The filtered acceleration spectrum was divided by the radian frequency to the fourth power to give a wave height spectrum [*Cartwright*, 1963]. The sum of the pitch spectrum and the roll spectrum constituted a spectrum of surface slope. Directional Fourier coefficients of the first two harmonics were calculated as given by *Longuet-Higgins et al.* [1963] and elaborated on by *Cartwright and Smith* [1964]. Directional parameters were calculated from the coefficients as was done in the previous section with radar measurements.

A sea sled provided measurements of pressure and horizontal water velocity components at a height of 1 m above the bottom [*Teleki et al.*, 1975]. A series of 4½-min records at different depths was used to generate spectra with 24 degrees of freedom. The mean water velocity varied between records, but values outside the surf line averaged about 10 cm/s to the south. A wave height spectrum was obtained from the 8.2-m depth pressure spectrum by using equations for linear waves [*Kinsman*, 1965], but only the low-frequency portion of this spectrum is considered to be accurate. The sum of the spectra of the two velocity components in that record was taken as an orbital velocity spectrum and corrected for depth. The mean direction $\bar{\theta}$ at each frequency was calculated from the spectra of velocity components as $\tan^{-1}(S_1(f)/S_2(f))^{1/2}$.

A second pressure sensor was mounted on a tower in shallow water operated through the University of Florida (see Figure 1). A combination of four short records taken during 3½ hours gave a pressure spectrum with about 22 degrees of freedom. The pressure spectrum was converted to a wave height spectrum as described above.

A Spectra Physics laser profilometer aboard the NASA CV-990 aircraft was operated farther offshore. Each record was processed with the assumption that the waves traveled in deep water in a single direction determined from the corresponding radar image [see *Long*, 1979]. Averages of spectra of contiguous records gave 56 and 98 degrees of freedom.

Figure 2 shows wave height spectra obtained from concurrent records from three of the reference instruments, and they seem to be in good agreement. Wave acceleration becomes small at low frequencies, and wave height spectra derived from acceleration records are less accurate in that frequency region. However, pressure-derived spectra are highly accurate in that region. The combined instruments provide an accurate representation of the wave conditions at the Marine-land site.

COMPARISONS OF WAVE HEIGHT SPECTRA

A normalized one-dimensional frequency spectrum derived from the radar image in Figure 1 is compared in Figure 3c with corresponding reference spectra of wave height, orbital velocity, and surface slope. The radar spectrum is a corrected version of that presented by *Shemdin et al.* [1978a] and *Teleki et al.* [1978]. Figures 4a and 4b contain spectra from two radar images at distances of 90 and 30 km from shore in water depths of 60 and 22 m, respectively, normalized to and compared with wave height spectra derived from the laser profilometer data. In each case the frequency of the peak of the radar spectrum is in good agreement with that of the wave height spectrum, although the frequency of the peak changed

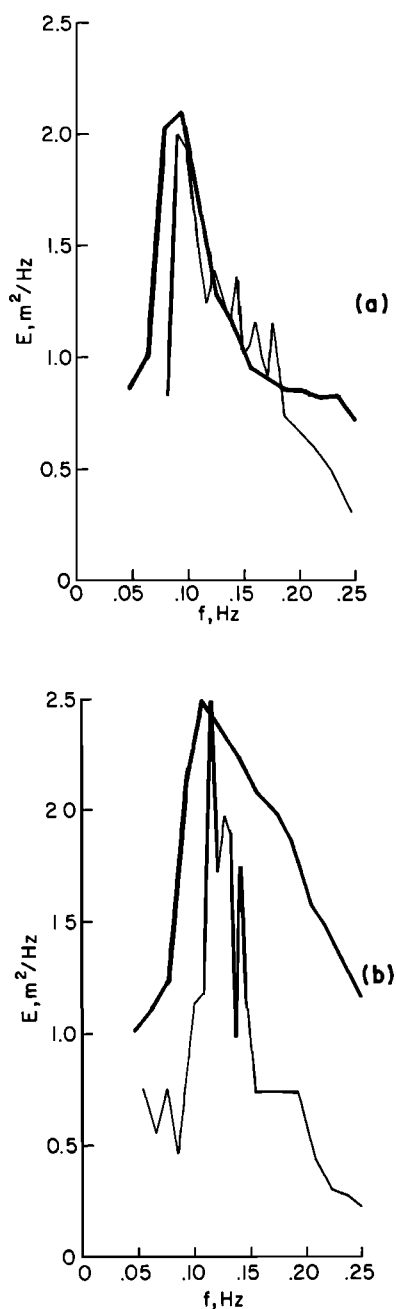


Fig. 4. Comparison of normalized radar spectra (heavy curves) at depths of (a) 60 m and (b) 22 m with the nearest laser profilometer wave height spectra (light curves). E is variance density.

with distance offshore. All of the spectra have steep slopes at lower frequencies.

The slope of the high-frequency portion of the radar spectrum in Figure 3 is much different from the same region of the surface slope spectrum. The radar slope will depend on the signal transfer function relating the data values used in the spectrum calculation to the original radar signal intensities. Since the photographic stages in the initial signal processing were not calibrated, it has not been possible to determine this relationship accurately. However, the difference in slope between the radar and surface slope spectra shows that the present radar images of large waves did not result predominantly from the slopes of those waves. Such a result might be expected with the large depression angles of the radar beam that

were used. Although the high-frequency portion of the radar spectrum in Figure 3 lies between the spectra of wave height and of orbital velocity, the high-frequency parts of the radar spectra in Figure 4 do not show a consistent relationship with the reference spectra. Nevertheless, the slope of this region of a radar spectrum generally does lie close to that of the wave height or orbital velocity spectrum, which suggests that a dependence on some aspect of the wave spectrum exists.

A few limited studies of the slopes of the high-frequency regions of radar wave spectra have been reported in the literature. In an early experiment, Myers [1958] compared spectra from vertically and horizontally polarized radar power signals with a wave height spectrum from a wave gage. The slopes in the high-frequency regions of the radar spectra varied considerably. In general, however, the vertically polarized radar spectra tended to lie close to the reference spectra, but the high-frequency portions of the horizontally polarized radar spectra decreased at a rate less steep than that of the reference. Zamarayev and Kalmykov [1969] considered that their non-scanned radar signals at a shallow depression angle represented the slopes of water waves traveling in one direction. A wave height spectrum derived from the radar matched a reference spectrum and supported their assumption of wave slope effects.

A single sea state will give radar wave height spectra with different high-frequency slopes under different operating conditions. The different conditions can call into play different mechanisms of radar response by ocean waves to much different extents. Within the range of variability that the differences between mechanisms introduce, the present wave height spectrum comparisons are considered to be consistent with the previous studies. However, the present spectra appear not to have been produced by a single mechanism, and the present limited comparison has not evaluated the mechanisms of radar return acting under these conditions.

WAVE DIRECTION MEASUREMENTS

Since the pitch-roll buoy cannot give directional spectra $E(\theta)$ directly, results from the buoy may be examined only with respect to directional wave models that are fit to the data. Two separate models are used: one derived from the pairs of coefficients of the first two harmonics of a directional Fourier transform $G(\theta)$ (Equation (9)) and one consisting of a cosine power function $P(f)$ (Equation (11)). For comparison with the buoy results, then, the radar data were calculated in terms of these two directional spread models.

In Figure 3b the mean wave directions $\bar{\theta}(f)$ derived from the radar image in Figure 1 through a partial directional Fourier transform (equations (7) and (10)) are compared with the corresponding values from the buoy and from the sea sled. The values from the different instruments are close at those frequencies where significant wave energy is shown in Figure 3c. At other frequencies, however, none of the three curves agree closely.

In Figure 3a the cosine power fit value $P(f)$ (Equation (11)) from the radar is in approximate agreement with the values from the buoy. The difference between the maximum values of 18 from the buoy and 12 from the radar may be attributed to a background noise in the radar data. Also, the directional spectrum $G(\theta)$ at 0.125 Hz reconstituted with Fourier coefficients from radar data near shore is in good agreement with the corresponding spectrum from the buoy (Figure 5). These

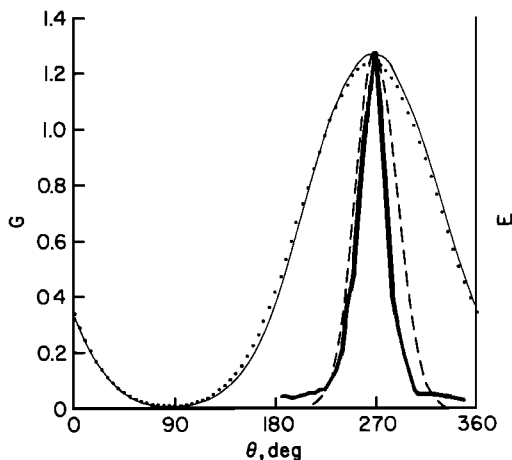


Fig. 5. Directional distribution of wave energy. The function $G(\theta)$ at 0.125 Hz was derived from the buoy (light solid curve) at 10-m depth and from the radar (dotted curve) at 14-m depth. E (dashed curve) was calculated from $P(0.125 \text{ Hz})$ derived from the buoy. The normalized energy distribution from the radar two-dimensional spectrum $S(k, \theta) = E$ (heavy solid curve), with the value of k for a frequency of 0.125 Hz, is shown for comparison.

comparisons demonstrate that radar can furnish directional distribution measurements of ocean waves equivalent to those from a buoy. In addition, to the extent that the two wave direction models that were used represent the ocean wave field the radar and the buoy appear to have recorded the waves similarly. *Shuchman and Zelenka* [1978] describe a possible directional variation in the transfer function relating radar measurements to ocean waves that would give an emphasis to waves traveling in the range direction. The comparisons indicate that such a directional variation must not have been great in the present radar measurements. Further evidence of the small directional variation of the transfer function in these radar data results from the observation that the radar directional spectra $E(\theta)$ in Figures 5 and 6 are approximately symmetrical even though the peaks of the directional spectra were 20° – 30° from the range direction.

The spread of a directional wave spectrum at one frequency may be characterized by a one-half power width representing the difference between the directions at which the energy density is one half of the maximum. Since the quantity $P(f)$ commonly is given as a representation of a directional spectrum of ocean waves, it might be expected that a one-half power width calculated with a value of $P(f)$ from the buoy would match the width observed directly from the radar spectrum. However, the maximum value of $P(f)$ from the buoy gives a width of 45° in Figure 5, while the radar peak $E(\theta)$ shows a width of 30° . That this difference may result from the procedure for calculating $P(f)$ is suggested by the calculation of a width of 55° with a value of $P(f)$ derived from the same radar data that show the 30° width in Figure 5. These greater widths of the fitted models are ascribed to the differences between the possible shapes of the two directional models and the actual wave directional spectrum. In particular, it appears that with narrow peaks the energy density at directions much different from the direction of the maximum can modify the value of $P(f)$ significantly. As a result the present observations provide an example in which the model-fitting techniques used for analysis of buoy data cannot fully describe the directional wave spectrum. In addition, the radar measurements allow a significantly greater directional resolution than do the buoy observations.

Directional properties of waves on the open ocean have been examined through buoy measurements in some previous studies. The directional widths varied with the state of development of the waves, but the widths were more consistent in a generating area than elsewhere and had minimum values at the frequencies of maximum wave energy. Maximum values of $P(f)$ have been reported for waves in a generating area in several of those studies: approximately 7 [*Longuet-Higgins et al.*, 1963], 13 [*Cartwright*, 1963], 16 [*Ewing*, 1969], and mostly less than 15 [*Mitsuyasu et al.*, 1975]. The present buoy data yield a maximum value of $P(f)$ of 18. Although the buoy measurements were obtained outside the wave-generating area, in shallow water, and near a shore, the radar directional distributions in Figure 6 show that the waves farther offshore and in the generating area also had narrow directional peaks. The narrow directional spectrum of waves shown by the radar can be understood only if either the buoy techniques do not fully describe the narrowness of wave directional spectra or the waves in the present study for some reason have a unique directional structure. *Tayfun et al.* [1976] calculated changes in the waves having a broad directional spectrum when they encountered a transverse current. The changes led to a sharp peak in the directional distribution. Satellite infrared observations show that the Gulf Stream was east of the locations of the present measurements [*Weissman et al.*, this issue]. If, indeed, waves in a generating area have a wide spread, it seems possible that the narrowness of the directional spectrum of the deepwater waves in Figure 6 should be attributed to refraction by an ocean current.

Tyler et al. [1974] obtained directional spectra of waves on the open ocean with a different synthetic aperture radar technique and examined the fine structure within their broad directional distributions. A particular lobe of energy within one range bin was not found to occur at a later time in the appropriate different range bin. In the data of Figure 6 the 60-m depth plot shows a minor lobe of wave energy propagating at about 30° to the right of the main peak, and this lobe is also apparent on the 22-m depth plot. Although the second lobe is

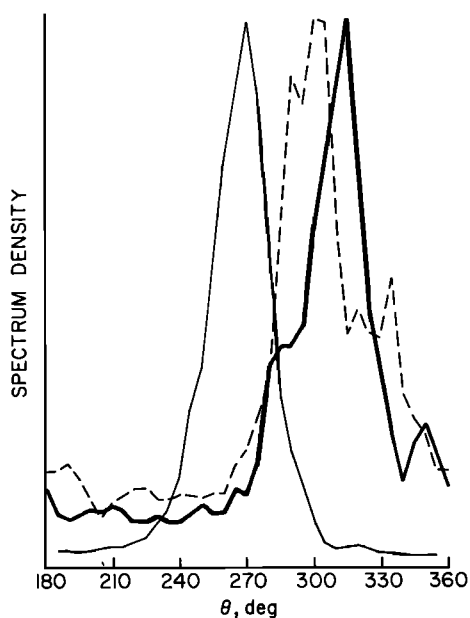


Fig. 6. Directional distribution of wave energy at 0.125 Hz from radar observations at depths of 60 m (heavy solid curve), 22 m (dashed curve), and 14 m (light solid curve). Amplitudes were adjusted to give the same energy at each peak.

not distinguishable from the main lobe nearer the shore, the occurrence of the second lobe at two locations 60 km apart suggests that it is not a random variation in the data. The ability of the present radar images to show wave trains at the same frequency but traveling in different directions is an improvement over the performance of other wave-recording instruments.

The directional spectra at 0.125 Hz from the radar image near shore were averaged at three different depths of water and are shown in Figure 7. The spectral amplitudes were not normalized. The energy distribution in the shallowest water was the narrowest, with a peak value 30% greater than the peak value in the deepest water. In contrast, the small amount of wave energy traveling more than 45° from the shoreward direction of 250° averaged about 30% less in the shallowest water than in the deepest water. The decrease is attributed to the turning of waves traveling largely along the coast toward the shore. The opposite directions of the two differences above cannot both be attributed to the methods of radar image formation or data processing, and the changes with depth appear to represent the effects of bottom refraction. The changes in mean direction shown in Figures 6 and 7 are not examined in this study.

The directional spreads of wave energy as indicated by $P(f)$ derived from three radar images at locations across the continental shelf are shown in Figure 8. There was insufficient wave energy at frequencies less than 0.07 Hz to allow interpretation of the spread calculations. Waves with frequencies greater than 0.14 Hz propagated mostly in deep water, and the spread did not change greatly across the shelf, except that waves in the lower frequencies show a narrower spread at a depth of 14 m. Since the water depths there were about 0.2 times the deepwater wavelength, the change may be attributed to bottom refraction.

In contrast to the directional narrowing near shore the waves with frequencies of 0.07–0.14 Hz show an increase in directional spread between depths of 60 and 22 m. The water depth varies from 0.07 to 0.75 times the deepwater length of these waves. It has been recognized that waves traveling in shallow water can be scattered in direction by irregularities in the bottom. *Oakley and Leverette* [1979] calculated that under possibly similar conditions of relative water depth and bottom roughness a narrow distribution in wave direction would be widened and the peak value would be reduced in energy by

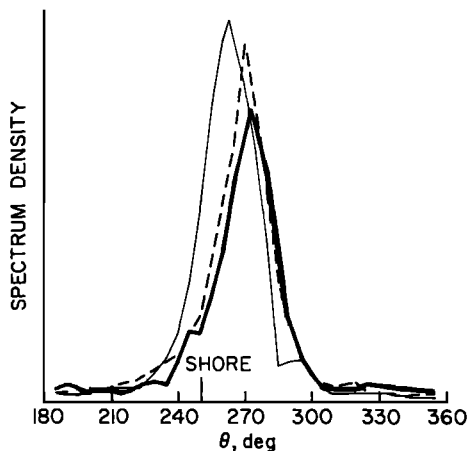


Fig. 7. Directional distribution of wave energy at 0.125 Hz at depths of 16 m (heavy solid curve), 14 m (dashed curve), and 12 m (light solid curve) in a single radar image. The amplitudes were not adjusted in this figure. The direction toward the shore was 250°.



Fig. 8. Cosine spreading exponent $P(f)$ from radar observations at depths of 60 m (heavy solid curve), 22 m (dashed curve), and 14 m (light solid curve). The maximum value of the 14-m plot (off scale) is 12.

one half because of bottom scattering while traveling only 12.5 km. The distance between the present radar images at 60- and 22-m depths is 60 km, and it appears that the widening of the directional spread of these waves might be attributed to bottom scattering. In addition, a comparison of Figures 3c and 4a shows that only 10% of the wave energy at 0.08 Hz survived the passage across the continental shelf. *Long* [1973] predicted that a scattering in direction of waves by bottom irregularities would eventually cause some energy to be scattered into an offshore direction and lead to a decrease in energy near shore. These data could be an observation of that effect. Other possible causes of the decrease in wave energy were discussed by *Hayes* [1977] and by *Shemdin et al.* [1978b].

CONCLUSIONS

Radar images of ocean waves gave values for the frequency and mean direction of the dominant waves in good agreement with reference measurements, although no wave height measurements from the radar were possible. An original goal of the Marineland experiment was to determine the mechanism of formation of radar patterns representing ocean waves by comparison with surface measurements [*Shemdin et al.*, 1975]. The determination was to be accomplished in part through comparison of the high-frequency slopes of the different spectra. Although the comparison showed that the effect of wave slopes was not the dominant mechanism of image formation under the present conditions, these data did not allow the mechanism to be specified further.

When the radar data were calculated in a manner parallel to that used for the buoy data, they gave a directional spectrum close to that from the buoy, except that the directions from the radar contained a 180° ambiguity. However, the radar directional distribution calculated directly had a peak much narrower than the peaks from the fitted models and showed the high directional resolution of the radar. This reso-

lution was apparent in two radar directional spectra that contained peaks in two different directions at a single frequency.

The differences between the fitted models and a directly calculated radar directional spectrum raises a possible question as to the appropriateness of current models in describing a directional distribution of waves on the open ocean. The present observations do not answer this question, but if previous measurements with fitted models do apply to unaltered ocean waves, the directional distribution of deepwater waves observed here may have been made narrower by a transverse ocean current. Waves in shallow water showed further directional narrowing that resulted from bottom refraction. The narrow directional distribution of a swell offshore became much wider as it traversed the continental shelf in relatively shallow water, apparently as a result of bottom scattering, and only a small fraction of its energy reached the coast.

The present observations strongly support the expectation that airborne radar accompanied by an independent airborne means of obtaining absolute wave height information (such as a pulsed radar altimeter or a laser profilometer that measures a one-dimensional wave height spectrum) can give complete two-dimensional spectra of ocean waves. These spectra could be obtained at a number of different locations nearly synoptically in a manner that seldom would be possible with in situ instrumentation.

Acknowledgments. Funds for this study were provided by the NOAA NESS Spacecraft Oceanography Project, the California Institute of Technology Jet Propulsion Laboratory, the Office of Naval Research, and the U.S. Army Corps of Engineers. Radar data were obtained and transformed to images by the Environmental Research Institute of Michigan. Digital values were obtained from the images and corrected for geometric distortion, and two-dimensional Fourier transforms were calculated at the Jet Propulsion Laboratory. The remaining calculations were performed at the Sea-Air Interaction Laboratory. Reference data were collected by the Sea-Air Interaction Laboratory, the U.S. Army Coastal Engineering Research Center, the University of Florida, and the NASA Ames Research Center. The authors are grateful to the many people who assisted in obtaining and processing the data used here. Particular thanks are due to Robert Berles, G. L. Howell, J. Losee, Frank Musialowski, Ron Peterson, R. Rawson, T. W. Thompson, and G. Tober.

REFERENCES

- Alpers, W. R., and C. L. Rufenach, The effect of orbital motions on synthetic aperture radar imagery of ocean waves, *IEEE Trans. Antennas Propagat.*, AP-27, 685-690, 1979.
- Bass, F. G., I. M. Fuchs, A. I. Kalmykov, I. E. Ostrousky, and A. D. Rosenberg, Very high frequency radiowave scattering by a disturbed sea surface, *IEEE Trans. Antennas Propagat.*, AP-16, 554-568, 1968.
- Bondarenko, I. M., A. A. Zagorodnikov, V. S. Loschilov, and K. B. Chelyshov, Relationship between wave parameters and the spatial spectrum of aerial photographs and radar pictures of the sea surface, *Oceanology*, Engl. Transl., 12, 912-919, 1972.
- Brown, W. M., and C. J. Porcello, An introduction to synthetic aperture radar, *IEEE Spectrum*, 6, 57-62, 1969.
- Cartwright, D. E., The use of directional spectra in studying the output of a wave recorder on a moving ship, in *Ocean Wave Spectra*, pp. 203-218, Prentice-Hall, Englewood Cliffs, N. J., 1963.
- Cartwright, D. E., and N. D. Smith, Buoy techniques for obtaining directional wave spectra, in *Buoy Technology*, pp. 112-121, Marine Technology Society, Washington, D. C., 1964.
- Crombie, D. D., Doppler spectrum of sea echo at 13.6 Mc/s, *Nature*, 175, 681-682, 1955.
- De Loor, G. P., and H. W. Brunsveld Van Hulst, Microwave measurements over the North Sea, *Boundary Layer Meteorol.*, 13, 119-131, 1978.
- Ewing, J. A., Some measurements of the directional wave spectrum, *J. Mar. Res.*, 27, 163-171, 1969.
- Gonzalez, F. I., R. C. Beal, W. G. Brown, P. S. DeLeonibus, J. W. Sherman III, J. R. R. Gower, D. Lichy, D. B. Ross, C. L. Rufenach, and R. A. Shuchman, Seasat synthetic aperture radar: Ocean wave detection capabilities, *Science*, 204, 1418-1421, 1979.
- Hayes, J. G., Ocean current and shallow water wave refraction in an operational spectral ocean wave model, *Tech. Note 77-1*, Fleet Number. Weather Cent., Monterey, Calif., 1977.
- Hsiao, S. V., The comparison between the synthetic aperture radar imageries and the surface truth of ocean waves, in *Ocean '78—The Ocean Challenge*, pp. 385-389, Marine Technology Society, Washington, D. C., 1978.
- Kinsman, B., *Wind Waves—Their Generation and Propagation on the Ocean Surface*, pp. 134 and 144, Prentice-Hall, Englewood Cliffs, N. J., 1965.
- Long, R. B., Scattering of surface waves by an irregular bottom, *J. Geophys. Res.*, 78, 7861-7870, 1973.
- Long, R. B., On surface gravity wave spectra observed in a moving frame of reference, *NOAA Tech. Memo. ERL AOML-38*, equations (6.9) and (6.13), U.S. Government Printing Office, Washington, D. C., 1979.
- Longuet-Higgins, M. S., D. E. Cartwright, and N. D. Smith, Observations of the directional spectrum of sea waves using the motion of a floating buoy, in *Ocean Wave Spectra*, pp. 111-132, Prentice-Hall, Englewood Cliffs, N. J., 1963.
- Mitsuyasu, H., F. Tasai, T. Suhara, S. Mizuno, M. Ohkusu, T. Honda, and K. Rikiishi, Observations of the directional spectrum of ocean waves using a Cloverleaf buoy, *J. Phys. Oceanogr.*, 5, 750-760, 1975.
- Myers, G. F., High-resolution radar, part IV, Sea clutter analyses, *Rep. 5191*, Naval Res. Lab., Washington, D. C., 1958.
- Oakley, O. H., Jr., and S. J. Leverette, Sea bottom spectra and ocean wave scattering, paper presented at BOSS '79 Conference, Mass. Inst. of Technol., London, Aug. 28-31, 1979.
- Rabiner, L. R., and B. Gold, *Theory and Application of Digital Signal Processing*, pp. 448-450, Prentice-Hall, Englewood Cliffs, N. J., 1975.
- Ross, D. B., B. Au, W. Brown, and J. McFadden, A remote sensing study of Pacific hurricane Ava, *Proc. Int. Symp. Remote Sensing Environ.*, 9th, 163-180, 1974.
- Shemdin, O. H., J. E. Blue, and J. A. Dunne, Seasat-A surface truth program: Marineland test plan, *Rep. 622-6*, Jet Propul. Lab., Pasadena, Calif., 1975.
- Shemdin, O. H., W. E. Brown, Jr., F. G. Staudhammer, R. Shuchman, R. Rawson, J. Zelenka, D. B. Ross, W. McLeish, and R. A. Berles, Comparison of in situ and remotely sensed ocean waves off Marineland, Florida, *Boundary Layer Meteorol.*, 13, 193-202, 1978a.
- Shemdin, O., K. Hasselmann, S. V. Hsiao, and K. Herterich, Non-linear and linear bottom interaction effects in shallow water, in *Turbulent Fluxes Through the Sea Surface, Wave Dynamics, and Prediction*, edited by A. Favre and K. Hasselmann, pp. 347-370, Plenum, New York, 1978b.
- Shuchman, R. A., and J. S. Zelenka, Processing of ocean wave data from a synthetic aperture radar, *Boundary Layer Meteorol.*, 13, 181-191, 1978.
- Tayfun, M. A., R. A. Dalrymple, and C. Y. Yang, Random wave-current interactions in water of varying depth, *Ocean Eng.*, 3, 403-420, 1976.
- Teleki, P. G., F. R. Musialowski, and D. A. Prins, Data acquisition methods for coastal currents, in *Proceedings of the Specialty Conference on Civil Engineering in the Oceans III*, pp. 1190-1210, American Society of Civil Engineers, New York, 1975.
- Teleki, P. G., W. McLeish, R. A. Shuchman, D. Ross, W. E. Brown, Jr., and M. Mattie, Ocean wave detection and direction measurements with microwave radar, in *Oceans '78—The Ocean Challenge*, pp. 639-648, Marine Technology Society, Washington, D. C., 1978.
- Teleki, P. G., W. J. Campbell, R. O. Ramseier, and D. Ross, The offshore environment: A perspective from Seasat SAR data, paper presented at Offshore Technology Conference, Houston, Tex., 1979.
- Tyler, G. L., C. C. Teague, R. H. Stewart, A. M. Peterson, W. H. Munk, and J. W. Joy, Wave directional spectra from synthetic aperture observations of radio scatter, *Deep Sea Res.*, 21, 989-1016, 1974.
- Weissman, D. E., T. W. Thompson, and R. Legeckis, Modulation of sea surface radar cross section by surface stress: Wind speed and

- temperature effects across the Gulf Stream, *J. Geophys. Res.*, this issue.
- Wright, J. W., A new model for sea clutter, *IEEE Trans. Antennas Propagat.*, AP-16, 217-223, 1968.
- Wright, J. W., T. R. Larson, and L. I. Moskowitz, A note on SAR imagery of the ocean surface, *IEEE Trans. Antennas Propagat.*, AP-24, 393, 1976.
- Zamarayev, B. D., and A. I. Kalmykov, On the possibility of determining the spatial structure of an agitated ocean by means of radar, *Izv. Acad. Sci. USSR. Atmos. Oceanic Phys.*, Engl. Transl., 5(1), 124-127, 1969.

(Received December 10, 1979;
revised March 28, 1980;
accepted April 4, 1980.)